Chemical Science

ROYAL SOCIETY OF CHEMISTRY

EDGE ARTICLE

View Article Online
View Journal | View Issue

Cite this: *Chem. Sci.*, 2025, **16**, 22119

All publication charges for this article have been paid for by the Royal Society of Chemistry

From surface-assisted synthesis of porous aromatic bulk sheets to readily assembled membranes for nanofiltration

Mengxiao Sun,† Geng Tan,† Zilong Dou, Jian Song, Xueting Qu, Yuyang Tian * and Guangshan Zhu *

Received 28th August 2025
Accepted 3rd October 2025

DOI: 10.1039/d5sc06612c

rsc.li/chemical-science

To address the challenges of global water scarcity and high energy consumption for water purification, nanofiltration by porous membranes provides a promising solution. The demand for precise pore modulation and enhanced stability in membranes renders porous organic frameworks (POFs) promising alternatives to polymeric membranes, as their intrinsic porosity can help overcome the typical selectivity-permeability trade-off. A key current goal is to synthesise POF membranes at size scales suitable for practical applications. Herein, a cost-effective and facile synthesis method is proposed to synthesize membranes comprising porous aromatic frameworks (PAFs), which are a class of porous frameworks with carbon-carbon-linked aromatic building units. Specifically, bulk PAF sheets are prepared on glass substrates by establishing noncovalent interactions between substrate hydroxyl groups and functional PAFs. A large number of PAF bulk sheets are directly synthesized on common substrates such as glass slides and silica wafers. These bulk sheets are readily assembled into membranes by spin coating. The obtained PAF membranes exhibit unprecedented nanofiltration performance, with water permeability up to 700 L m^{-2} h^{-1} MPa^{-1} and rejection above 99% for the organic dye Congo Red. This surface-assisted synthesis and assembly of PAF membranes represent a step forward in the fabrication of porous organic separating membranes.

Introduction

Global water contamination and unsustainable water consumption related to urban wastewater, rivers and seawater represent increasing challenges, and the need for safe water has stimulated continuous advancements in water purification technologies in recent years.[1,2] When considering both capital and energy consumption, membrane technology offers distinct advantages for clean water demands.[3–5] Microporous membranes comprising nanoporous materials possess opening windows on the molecular scale and have therefore attracted extensive attention for size-dependent filtration.[6–8] In contrast to polymeric membranes and mixed matrix membranes (MMMs) with porous materials embedded in a polymeric matrix, continuous microporous membranes exhibit penetrating channels and defect-free texture.[9,10] Therefore, they show high selectivity and high permeating flux at the same time in the separation process. To date, microporous membranes based on various porous materials including zeolites,[11,12] metal organic frameworks (MOFs)[13–15] and covalent organic frameworks (COFs)[16–18] have been widely reported. The formation of these polycrystalline membranes relies on heterogeneous growth at the substrate surfaces.[19] To achieve large-area and defect-free membranes, preferred interactions between crystals and the substrate surface should be established, and subtle control of the synthesis process is required.[20] Meanwhile, these polycrystalline membranes suffer from high brittleness and relatively low stability in harsh environments, because the crystals are grown *via* reversible bond formation.[21,22] In contrast, porous organic frameworks—entirely composed of organic building units—have experienced rapid developments in the past decade and can overcome the limitations in stability and structural modification of crystalline porous materials. Porous aromatic frameworks (PAFs) are representative of these porous organic materials. They are formed from building units with rigid benzene rings and synthesized *via* irreversible coupling reactions, which provide them with tough carbon–carbon linkages.[23,24] PAFs are famous for their advantages, including high specific surface area, inherent porosity and structural adjustability, and can withstand harsh environmental conditions, such as acids, alkalis, high salt and high humidity.[25,26]

The preparation of continuous PAF membranes overcomes the limitations of crystalline microporous membranes in terms of performance regulation and stability, and therefore, they are considered potential candidates for separating membranes.[27] Although a few PAF membranes have been synthesized by covalent bonding on smooth surfaces with anchoring sites, studies have shown that it is still a challenge to achieve growth

Key Laboratory of Polyoxometalate and Reticular Material Chemistry of Ministry of Education, Faculty of Chemistry, Northeast Normal University, Changchun, Jilin 130024, China. E-mail: tianyy100@nenu.edu.cn; zhugs@nenu.edu.cn

† These authors contributed equally to this work.

control for PAFs from powder compounds to a two-dimensional layered morphology. This is mainly because PAFs are insoluble frameworks due to the high irreversibility of the non-dynamic chemical bond formation process.[28] In previous work, we successfully synthesized a continuous PAF membrane for gas separation using a surface-initiated strategy.[9] Covalent bonds were formed between PAF membranes and substrate surfaces. The key to the success of the surface-initiated strategy is modifying an active site that covalently binds to PAFs on the substrate surface, and multi-step reactions and modifications are required to achieve specific and high-density modification of the active sites. The complex surface initiation process is currently the main impediment to the successful synthesis of continuous PAF membranes on a large scale. To solve this problem, there is an urgent need to develop a universally applicable, simple and cost-effective method for PAF membrane preparation, in contrast to the previously used surface-initiated strategy.

Glass substrates and other oxide surfaces are commonly used in laboratories and production factories, and direct growth of PAF membranes at these surfaces would be attractive for the fabrication process. Considering the surface chemistry, there are abundant hydroxyl groups at the surfaces of glass and other oxide substrates. Unlike establishing covalent bonds on substrate surfaces, it would be an efficient and simple synthetic method to prepare PAF films by constructing noncovalent interactions directly with hydroxyl functional groups. Herein, PAF bulk sheets on the millimeter scale are directly synthesized on general substrates like glass slides, silica wafers, or even the inner walls of glass containers without extra modifications. It is found that noncovalent interactions between PAFs and substrates play an important role in the successful growth and morphology control for flake-like PAFs. Building units of PAFs with hydroxyl groups are necessary, and the results indicate that the interaction between PAF building units and hydroxyl-containing substrates contributes to the simple and large-scale synthesis of PAF bulk sheets, and finally leads to a series of large-size continuous PAF membranes as a result of their assembly.

The self-assembled PAF membranes exhibit unprecedented water permeability as high as 700 L m^{-2} h^{-1} MPa^{-1} and over 99% retention for the organic dye Congo Red (CR). In this study, noncovalent interactions are crucial to trigger the surface growth, which reduces the manufacturing cost of PAF membranes, improves the yield of layered PAFs, and solves the major problems that otherwise hinder the development of low-cost, large-size separating membranes. The study provides important concepts and strategies for the preparation of a wide range of PAF membranes with high performance, and promotes the development of continuous PAF membranes with functional tunability for water purification.

Results and discussion

Fabrication and characterization of PAF-80 bulk sheets on glass slides

Glass slides were treated by oxidation and had rich hydroxyl groups at the surfaces; therefore, PAFs with hydroxyl functional groups could establish noncovalent interactions with the glass substrates. PAF-80 bulk sheets were successfully obtained on the surface of glass slides with building units. In PAF-80, the framework consists of two building units: 1,3,5-triethynylbenzene (TEB) and 2,4,6-tribromobenzene-1,3,5-triol (TBBT). Due to the van der Waals interactions between phenolic hydroxyl groups in TBBT and hydroxyl groups on the glass surface, the growth of PAF bulk sheets on the glass

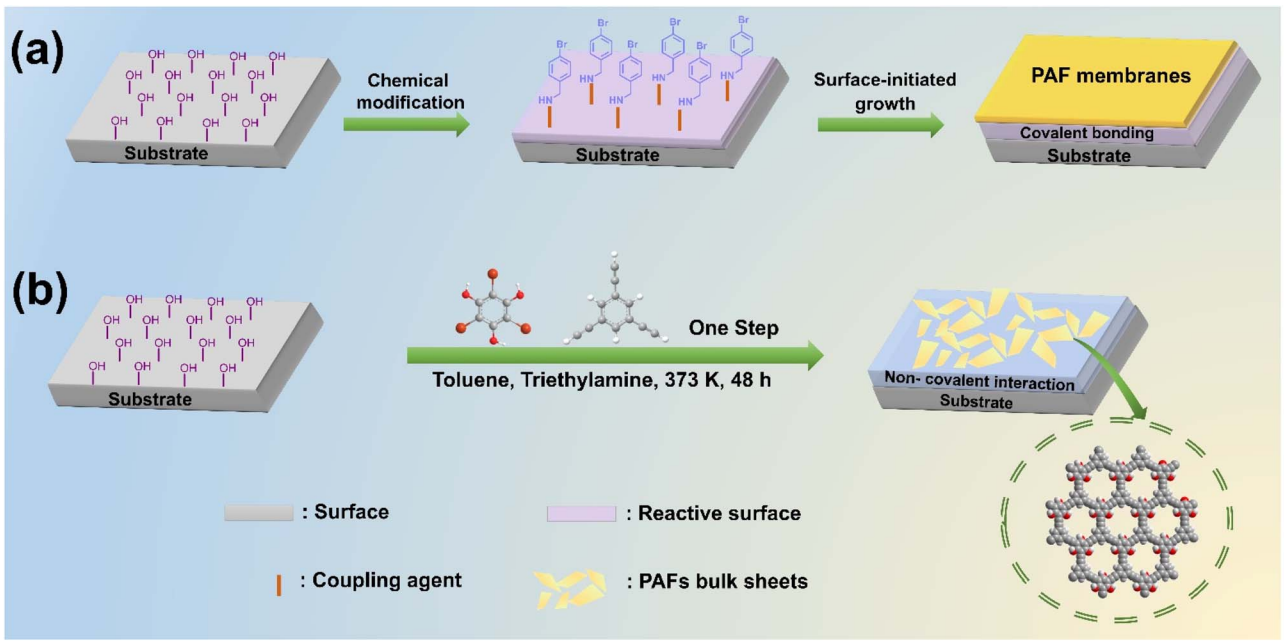

Fig. 1 Membrane fabrication process. (a) Schematic illustration of the fabrication process of a PAF continuous membrane based on the surface-initiation strategy; (b) schematic illustration of the fabrication process of PAF bulk sheets based on non-bonding interactions.

substrates was readily achieved, without any further chemical modification of the glass slides, in turn reducing the cost of PAF sheet growth (Fig. 1).

The PAF-80 bulk sheets were successfully synthesized on the glass surface, as observed by the color change of the transparent glass slides. They were then stripped from the surface of the glass substrate by simple ultrasonication (Fig. 2b), and the size and shape of the PAF bulk sheets were derived from the glass substrate. The synthetic process was monitored using Fourier-transform infrared (FT-IR) spectroscopy. The changes in the spectra showed the successful growth of PAF-80 on the glass slides, evidenced by the disappearance of the vibration at 3282 cm^{-1} originating from the terminal alkyne group in TEB, and the disappearance of the vibration at 1068 cm^{-1} from the C–Br bond in TBBT. At the same time, the low-intensity bands at 2200 cm^{-1} for the synthesized PAF-80 were assigned to the stretching vibration modes of the alkyne (C≡C) moieties.[29] All these results indicated the synthesis of PAF-80 in the expected way. The wide infrared band at 3440 cm^{-1} could be attributed to a tensile vibration of the hydroxyl group (–OH), indicating that the hydroxyl group remained after the coupling reaction. The main characteristic peaks of PAF-80 powder and PAF-80 sheets were consistent, thus demonstrating the successful synthesis of PAF-80 bulk sheets (Fig. 2c and S1). The integrity of the PAF-80 bulk sheets on the substrate was characterized using scanning electron microscopy (SEM), and no significant cracks or pore defects were observed (Fig. 2d and S2). Energy dispersive spectroscopy (EDS) elemental mapping of PAF-80 sheets on the glass substrate showed a continuous and homogeneous carbon distribution (Fig. S3). The microscopic morphology of the PAF-80 sheets was characterized by transmission electron microscopy (TEM), and the sheets showed two-dimensional silk-like

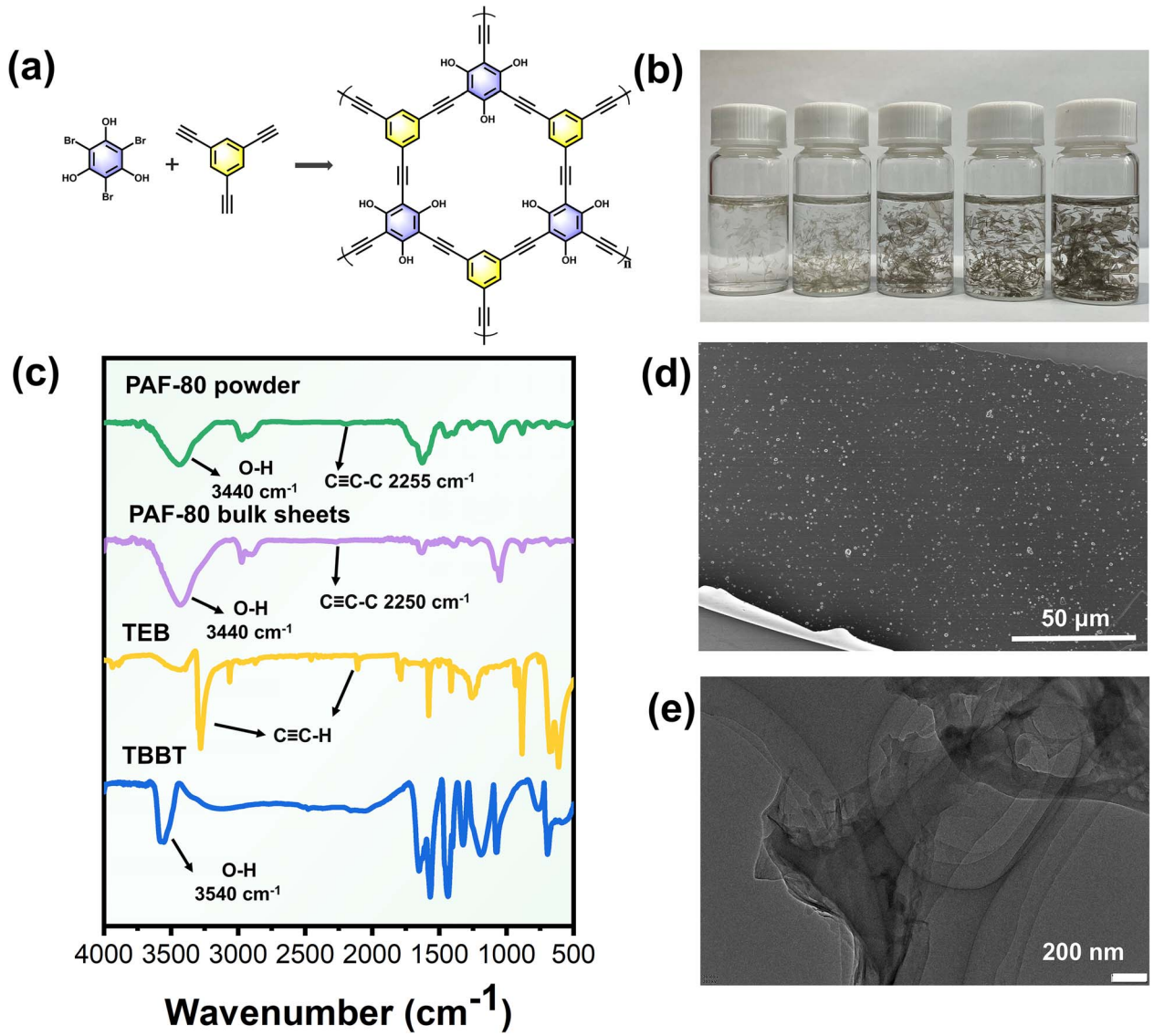

Fig. 2 Morphologies and physicochemical properties of PAF-80 bulk sheets. (a) Structural design of the PAF-80 bulk sheets; (b) optical photograph of the PAF-80 bulk sheets with different growth times: from left to right 6 h, 12 h, 24 h, 48 h and 72 h; (c) FT-IR spectra of the PAF-80 bulk sheets; (d) SEM image of the PAF-80 bulk sheets; (e) TEM image of the PAF-80 bulk sheets.

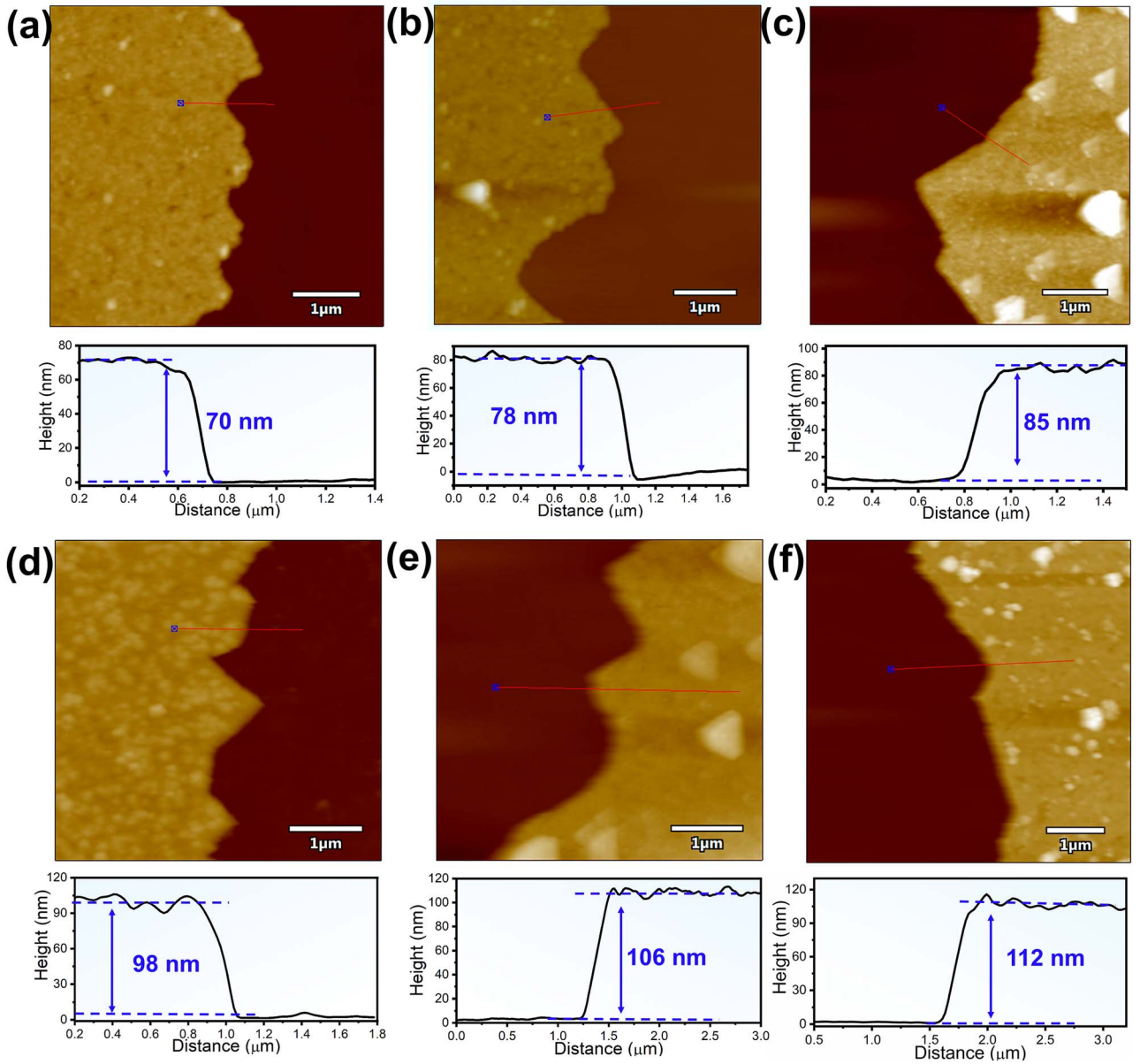

Fig. 3 AFM images of the surface morphologies of PAF-80 sheets at different growth times. In order to facilitate AFM testing, PAF-80 sheets were grown in the same way after simple oxidation treatment on a silicon wafer substrate. (a) 6 h; (b) 12 h; (c) 24 h; (d) 48 h; (e) 72 h; (f) 96 h.

texture with stacked layers (Fig. 2e and S4). Atomic force microscopy (AFM) was used to evaluate the thickness and roughness of the PAF-80 sheets. The thickness changes of the PAF-80 sheets at different time intervals were also monitored by AFM to investigate the growing progress (Fig. 3). The AFM images showed that a continuous layer was formed on the surface of the substrates after 6 hours, with a thickness of about 70 nm, and the surface of the layer was smooth and particle-free (Fig. 3a). After 24 h, the thickness of the layer increased to 85 nm, and a small number of accumulated particles could be observed atop the layer (Fig. 3c). After 96 h of reaction, the thickness of the layer reached 112 nm, and a significantly rough surface was observed, which may be formed by the accumulation of PAF particles on the sheet surface (Fig. 3f). The growing thickness of the layer linearly increased over time, suggesting an epitaxial growing mechanism for the formation of an amorphous layer on a flat surface (Fig. S5). Usually, PAFs from aromatic building units show extreme hydrophobicity, which results in diminished water permeation across their pores. Herein, the water compatibility of the PAF-80 sheets was monitored by water contact angle testing. As the growth time increased, the water contact angle gradually became smaller, demonstrating that the PAF-80 sheets became more hydrophilic due to the presence of hydroxyl groups. The hydrophilic sheets were promising to enhance the water permeability (Fig. S6). X-ray photoelectron spectroscopy (XPS) results indicated that

the surface of the PAF-80 bulk sheet is exposed to abundant hydroxyl groups (Fig. S7).

During the synthesis process of PAF-80 sheets with different growth times, it was found that PAF powder was also present in the reaction system but could be removed, while the membranes were attached to the surface of the substrates and even the reaction vials (Fig. S8). In this case, the attached bulk sheets and free PAF powder were readily isolated by washing. Following ultrasonication, the large-area membranes were successfully detached from the substrates and transferred to the vial (Fig. S9–11). We propose that this phenomenon can be attributed to supramolecular interactions driven by surface interface chemistry. Specifically, hydroxyl groups on the glass substrates likely formed noncovalent bonds with the structural units of the PAF-80 bulk sheets. Although individual supramolecular interactions were relatively weak, their collective synergistic effect enabled the growth of extensive PAF-80 bulk sheets along the substrates.

Verifying the universality of the method

To verify the generality of the method, other PAF sheets were synthesized on glass substrates using TBBT coupled with alkyne-based building units, such as 1,4-diethylbenzene (DTB), tetrakis(4-ethynylphenyl)benzene (TEPB), and tetrakis(4-ethynylphenyl)methane (TEPM). The obtained bulk sheets were named PAF-81, PAF-82, and PAF-18, respectively. Optical images confirm that PAF sheets can be prepared on the substrates by designing the structure of the PAFs to establish noncovalent interaction, and high yields of bulk sheet preparation were achieved (Fig. 4a–c). From the SEM, TEM and AFM results, it could be seen that PAF-81 sheets, PAF-82 sheets and PAF-18 sheets were successfully synthesized (Fig. S12–S22). The AFM images and measurements showed that the thickness varied from 10 nm to 100 nm (Fig. 4d–f). It was found that only building units with hydroxyl groups could form bulk sheets on glass substrates or silica wafers, indicating the crucial role of noncovalent interaction for PAF growth at the substrate surfaces.

Preparation and nanofiltration performance of the PAF-80 membrane. With the development of the printing and dye industry, organic dyes are used in large quantities and dye effluent is discharged into water in the environment.[10,30] Congo red (CR) is in the group of azo compounds, which are highly toxic as well as carcinogenic. The presence of aromatic amine groups makes it difficult for them to biodegrade.[31] Therefore, the ability to effectively remove CR dye from wastewater has enormous benefits for human health.

A homemade pressure-assisted filtration device (Fig. S25) was used to test the flux of pure water through the PAF

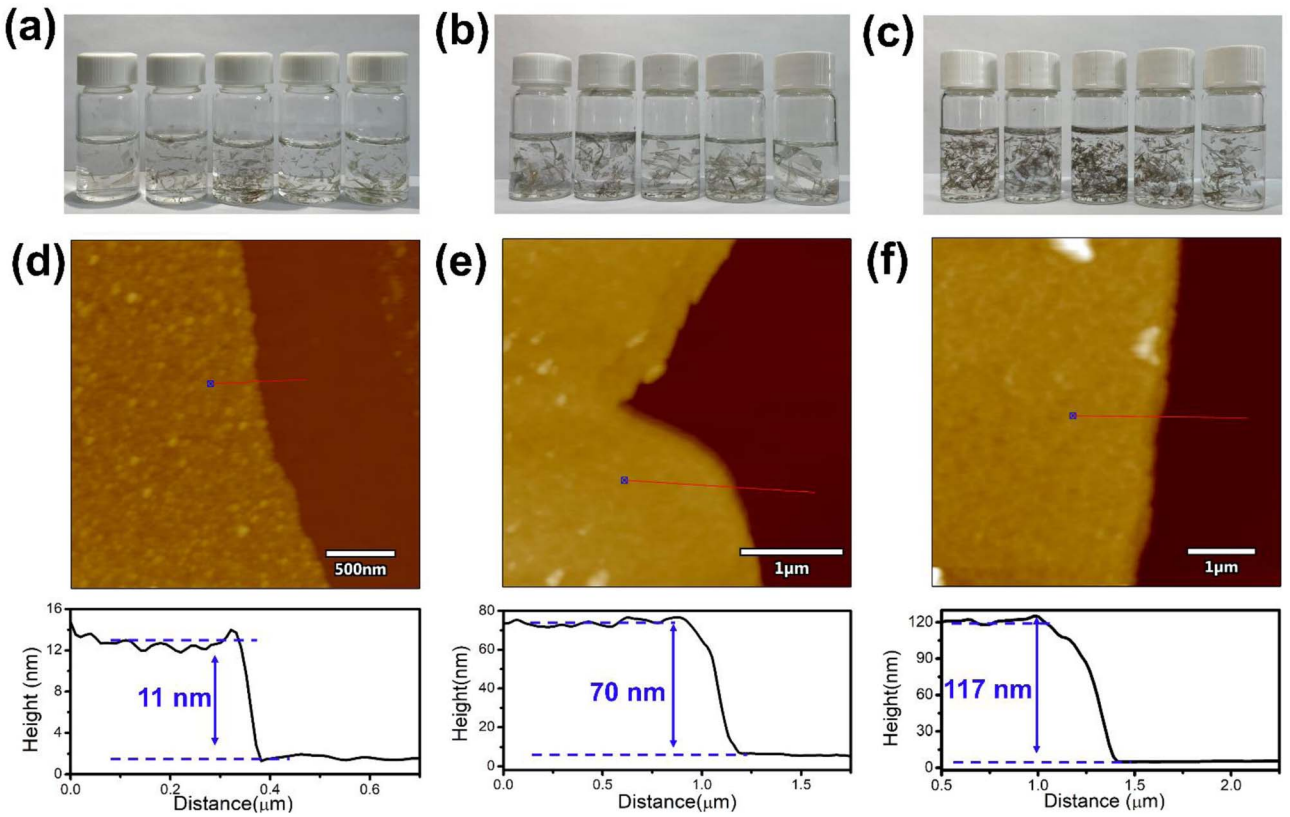

Fig. 4 Optical photographs of PAF sheets with different growth times on a glass substrate, from left to right: 6 h, 12 h, 24 h, 48 h, 72 h. (a) PAF-81 bulk sheets; (b) PAF-82 bulk sheets; (c) PAF-18 bulk sheets. (d) PAF-81 sheets grown for 48 h after simple oxidation treatment on a silicon wafer substrate; (e) PAF-82 sheets grown for 48 h after simple oxidation treatment on a silicon wafer substrate; (f) PAF-18 sheets grown for 48 h after simple oxidation treatment on a silicon wafer substrate.

membranes and the separation performance of the membranes for aqueous solutions of Congo Red (CR). The concentration of the aqueous CR solution was 100 mg L^{-1}, and the working pressure of the device could be adjusted using a pressure gauge. Before the formal test, the continuous PAF membranes were pressurized with pure water at 0.2 MPa for 2 h to ensure stable permeability, and then the pure water flux and dye separation performance of the continuous PAF membrane were tested under 0.1 MPa conditions, and the subsequent permeate was collected after discarding the initial 1 h permeate. Determination of the feed and osmotic concentration of the aqueous CR solution was carried out using a UV-vis spectrophotometer. Two important parameters for evaluating the performance of PAF membranes were permeability (P) and rejection rate (R), determined by the following equations:

$$P = \frac{V}{tA\Delta P}$$

where V is the volume of the permeation solution (L), t is the sample collection time (h), A is the effective membrane area (m^2), and ΔP is the applied transmembrane pressure (MPa),[32] and:

$$R = 1 - \frac{C_p}{C_f}$$

where C_p and C_f are the concentrations of the solution in the permeate and feed solution, respectively.

After obtaining the PAF bulk sheets, the nanofiltration performance of four types of PAF bulk sheets was first tested and evaluated. The separation results are shown in Fig. S27 and Table S2. To fully achieve nanofiltration membranes for water purification, PAF-80 bulk sheets were dispersed in a chlorobenzene solution of PMMA and prepared as large-size membranes using the spin-coating method (Fig. 5a and b). SEM confirmed the continuity of the PAF-80 membranes and the uniform distribution of the elements (Fig. 5c, d and S28). The thickness of the PAF-80 membrane was increased very little, maintaining 113 nm (Fig. S28).

The nanofiltration performance of PAF-80 membranes for aqueous CR solutions was tested and evaluated (Fig. 5e–g). The water flux through the PAF-80 membrane can be stabilized above 700 L m^{-2} h^{-1} MPa^{-1}, and the retention rate of CR reached 99.9%. Moreover, even after five nanofiltration cycles, the membrane can still achieve a permeation flux of over 700 L

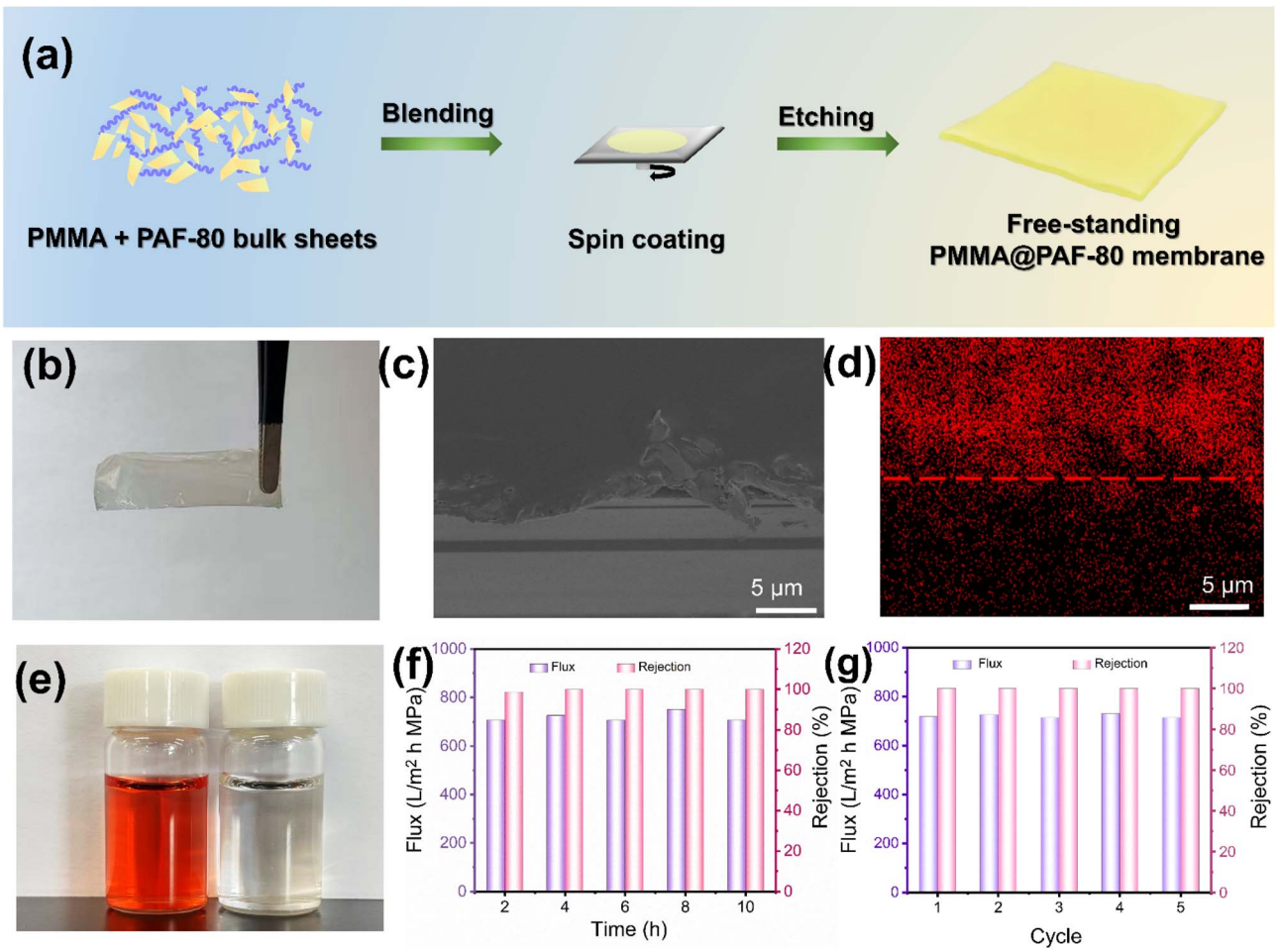

Fig. 5 Preparation and performance study of the PAF-80 nanofiltration membrane. (a) Preparation process; (b) optical photograph of the PMMA@PAF-80 independent membrane; (c) SEM image and (d) carbon element distribution of the PMMA@PAF-80 membrane on the silicon wafer before etching; (e–g) nanofiltration performance.

m^{-2} h^{-1} MPa^{-1} and a rejection rate of 99.9% (Table S3). The separation performances of the PAF-81 membrane, PAF-82 membrane and PAF-18 membrane were investigated under the same testing conditions. The separation results are shown in Fig. S29 and Table S4. The zeta potential results indicate that PAF-80 possesses a negative surface charge, while CR is also negatively charged. Therefore, no electrostatic interaction exists between PAF-80 and CR (Fig. S30). The high retention was caused by the size sieving effect of the porous aromatic sheets. As calculated by NLDFT simulation according to the nitrogen adsorption isotherm, the pore size of PAF-80 was centered at 0.52 nm (Fig. S31), which is smaller than the molecular dimension of CR.[33] Combining the analysis of the PAF-80 membrane skeleton structures with experimental results reveals that PAF-80 membranes contain hydroxyl functional groups, which readily allow adjustment of membrane surface properties to achieve high water flux and high CR molecular rejection. PAF membranes are expected to achieve the separation of CR molecules in wastewater with the actual water flux and good rejection rate (Table S5).

Experimental methods

Supramolecular interaction force-initiated polymerization (synthesis of PAF-80 bulk sheets)

A glass slide was immersed in piranha liquid for 8 h, then washed using distilled water and ultrapure water, and flow-dried with high-purity nitrogen. The washed glass slide was put into a mixture of anhydrous toluene and triethylamine at 100 °C and activated for 1 h, and a volume of 20 mL (1 : 1 vol) of tetrakis(triphenylphosphine) palladium (0.012 mmol, 13.8 mg) and CuI (0.012 mmol, 2.3 mg) was added to the mixture. TEB (0.1 mmol, 15 mg) and TBBT (0.1 mmol, 36.3 mg) were added to the reaction system, and the operating environment was all nitrogen. The reaction was carried out at 100 °C for 48 h. At the end, the reaction was cooled to room temperature, and the glass slide was washed with trichloromethane and anhydrous methanol.

Supramolecular interaction force-initiated polymerization (synthesis of PAF-81 bulk sheets)

A washed glass slide was put into a mixture of anhydrous toluene and triethylamine at a volume of 20 mL (1 : 1 vol). Tetrakis(triphenylphosphine)-palladium (0.012 mmol, 13.8 mg) and CuI (0.012 mmol, 2.3 mg) were added to the mixture and activated at 100 °C for 1 h. DTB (0.1 mmol, 18.9 mg) and TBBT (0.1 mmol, 36.3 mg) were added to the reaction system, and the operating environment was all nitrogen. The reaction was carried out at 100 °C for 48 h. At the end, the reaction was cooled to room temperature, and the glass slide was washed with trichloromethane and anhydrous methanol.

Supramolecular interaction force-initiated polymerization (synthesis of continuous PAF-82 bulk sheets)

A washed glass slide was put into a mixture of anhydrous toluene and triethylamine at a volume of 20 mL (1 : 1 vol). Tetrakis(triphenylphosphine)-palladium (0.012 mmol, 13.8 mg) and CuI (0.012 mmol, 2.3 mg) were added to the mixture and activated at 100 °C for 1 h. TEPB (0.1 mmol, 37.85 mg) and TBBT (0.1 mmol, 36.3 mg) were added to the reaction system, and the operating environment was all nitrogen. The reaction was carried out at 100 °C for 48 h. At the end, the reaction mixture was cooled to room temperature, and the glass slide was washed with trichloromethane and anhydrous methanol.

Supramolecular interaction force-initiated polymerization (synthesis of PAF-18 bulk sheets)

A washed glass slide was put into a mixture of anhydrous toluene and triethylamine at a volume of 20 mL (1 : 1 vol). Tetrakis(triphenylphosphine)-palladium (0.012 mmol, 13.8 mg) and CuI (0.012 mmol, 2.3 mg) were added to the mixture and activated at 100 °C for 1 h. TEPM (0.1 mmol, 31.24 mg), and monomer 2 (0.1 mmol, 36.3 mg) were added to the reaction system, and the operating environment was all nitrogen. The reaction was carried out at 100 °C for 48 h. At the end, the reaction was cooled to room temperature, and the glass slide was washed with trichloromethane and anhydrous methanol.

Conclusions

In this work, a simple protocol for the synthesis of PAF sheets on common hydroxyl-containing substrates was developed. Noncovalent interaction was crucial to trigger the surface growth, which reduced the manufacturing cost of the PAF sheets, improved the yield of layered PAFs, and solved the major problems in the development of low-cost, large-size membranes. PAF-80 bulk sheets, PAF-81 bulk sheets, PAF-82 bulk sheets, and PAF-18 bulk sheets were successfully prepared. These bulk sheets, synthesized at a large scale and in high yield, were readily assembled into membranes through spin coating, delivering high rejection rates for nano-sized dyes with high water flux and excellent stability.

Author contributions

Guangshan Zhu and Yuyang Tian conceived and supervised the project. Mengxiao Sun designed and carried out the experiments, analyzed the data, and wrote the manuscript. Geng Tan, Zilong Dou, Jian Song and Xueting Qu participated in material synthesis and characterization. All authors discussed the results and commented on the manuscript.

Conflicts of interest

There are no conflicts to declare.

Data availability

The data supporting this article have been included as part of the supplementary information (SI). Supplementary information: additional experimental details, materials characterization

data (*e.g.*, SEM, TEM, and BET analysis), and supplementary nanofiltration performance results. See DOI: **https://doi.org/10.1039/d5sc06612c**.

Acknowledgements

This work was financially supported by the Science and Technology Research Project of Education Department of Jilin Province (JJKH20241417KJ). The authors are grateful for financial support from the National Natural Science Foundation of China "111" project (no. B18012).

References

1 J. Fei, W. Sun, H. Li, Z. Mo, Q. She, X. Yang, T. Huang, M. Fang, Z. Wang, S. D. Snow and X. Zhu, *Environ. Sci. Technol.*, 2025, **59**, 11907–11918.
2 Y. Guo and G. Yu, *ACS Mater. Lett.*, 2022, **4**, 713–714.
3 L. Nie, C. Y. Chuah, T. H. Bae and J. M. Lee, *Adv. Funct. Mater.*, 2021, **31**, 2006949.
4 Y.-S. Jun, X. Wu, D. Ghim, Q. Jiang, S. Cao and S. Singamaneni, *Acc. Chem. Res.*, 2019, **52**, 1215–1225.
5 G. M. Shi, Y. Feng, B. Li, H. M. Tham, J.-Y. Lai and T.-S. Chung, *Prog. Polym. Sci.*, 2021, **123**, 101470.
6 L. Nie, K. Goh, Y. Wang, J. Lee, Y. Huang, H. E. Karahan, K. Zhou, M. D. Guiver and T.-H. Bae, *Sci. Adv.*, 2020, **6**, eaaz9184.
7 C. Cheng, S. A. Iyengar and R. J. N. N. Karnik, *Nat. Nanotechnol.*, 2021, **16**, 989–995.
8 Y. Liang, Y. Zhu, C. Liu, K.-R. Lee, W.-S. Hung, Z. Wang, Y. Li, M. Elimelech, J. Jin and S. Lin, *Nat. Commun.*, 2020, **11**, 2015.
9 Y. Ma, F. Cui, H. Rong, J. Song, X. Jing, Y. Tian and G. Zhu, *Angew. Chem., Int. Ed.*, 2022, **61**, e202113682.
10 H. Fan, J. Gu, H. Meng, A. Knebel and J. Caro, *Angew. Chem., Int. Ed.*, 2018, **57**, 4083–4087.
11 Y. Deng, F. Qiu, J. Wu, J. Li, Z. Li, Q. Huang, G. Zhu and X. Zou, *Angew. Chem., Int. Ed.*, 2025, **64**, e202421285.
12 D. Fu, J. E. Schmidt, P. Pletcher, P. Karakiliç, X. Ye, C. M. Vis, P. C. A. Bruijnincx, M. Filez, L. D. B. Mandemaker, L. Winnubst and B. M. Weckhuysen, *Angew. Chem., Int. Ed.*, 2018, **57**, 12458–12462.
13 Z. Liu, J. Chu, L. Cheng, J. Wang, C. Zhang, C. Zhang, F. Cui, H. Wang and G. Zhu, *Chem. Sci.*, 2025, **16**, 2810–2818.
14 H. Yuan, K. Li, D. Shi, H. Yang, X. Yu, W. Fan, P. J. S. Buenconsejo and D. Zhao, *Adv. Mater.*, 2023, **35**, 2211859.
15 D. Shi, X. Yu, W. Fan, V. Wee and D. Zhao, *Coord. Chem. Rev.*, 2021, **437**, 213794.
16 H. Jiang, C. Cao, W. Liu, H. Zhang, Q. Li, S. Zhu, X. Li, J. Li, J. Chang, W. Hu, Z. Xing, X. Zou and G. Zhu, *J. Energy Chem.*, 2025, **104**, 127–135.
17 Y. H. Jin, M. H. Li and Y. W. Yang, *Adv. Sci.*, 2025, **12**, 2412600.
18 M. B. Asif, S. Kim, T. S. Nguyen, J. Mahmood and C. T. Yavuz, *J. Am. Chem. Soc.*, 2024, **146**, 3567–3584.
19 H. Yang, J. Xu, H. Cao, J. Wu and D. Zhao, *Nat. Commun.*, 2023, **14**, 2726.
20 F. Dorosti, L. Ge, H. Wang and Z. Zhu, *Prog. Mater. Sci.*, 2023, **137**, 101123.
21 B. Hosseini Monjezi, K. Kutonova, M. Tsotsalas, S. Henke and A. Knebel, *Angew. Chem., Int. Ed.*, 2021, **60**, 15153–15164.
22 L. Ren, H. Wu, J. Han and J. Chen, *Adv. Funct. Mater.*, 2025, **35**, 2425244.
23 Y. Tian and G. Zhu, *Chem. Rev.*, 2020, **120**, 8934–8986.
24 Y. Yuan and G. Zhu, *ACS Cent. Sci.*, 2019, **5**, 409–418.
25 Y. Tian, F. Cui, Z. Bian, X. Tao, H. Wang, N. Zhang and G. Zhu, *Acc. Chem. Res.*, 2024, **57**, 2130–2143.
26 H. Lei, Z. Zhang, Y. Zhai, X. Han, J. Song, Y. Li and Y. Tian, *Chem. Synth.*, 2024, **4**, 62.
27 M. Ratsch, C. Ye, Y. Yang, A. Zhang, A. M. Evans and K. Borjesson, *J. Am. Chem. Soc.*, 2020, **142**, 6548–6553.
28 H. Ali, Y. Orooji, A. Y. A. Alzahrani, H. M. Hassan, Z. Ajmal, D. Yue and A. Hayat, *ACS Nano*, 2025, **19**, 7482–7545.
29 M. Chen, F. Muhammad, A. Saba, J. Song, X. Wang, Y. Tian, S. Ding and G. Zhu, *RSC Adv.*, 2020, **10**, 26335–26341.
30 C. Shi, C. Lv, L. Wu and X. Hou, *J. Hazard. Mater.*, 2017, **338**, 241–249.
31 V. Selvaraj, T. S. Karthika, C. Mansiya and M. Alagar, *J. Mol. Struct.*, 2021, **1224**, 129195.
32 C. Chen, J. Wang, D. Liu, C. Yang, Y. Liu, R. S. Ruoff and W. Lei, *Nat. Commun.*, 2018, **9**, 1902.
33 L. Y, Y. Yang, T. Chu, H. Niu, J. Wang and Y. Cai, *Nat. Commun.*, 2022, **13**, 2615.